Interaction Field Based and Hologram Based QSAR Analysis of Propafenone-type Modulators of Multidrug Resistance

D. Kaiser[a], M. Smiesko[a], S. Kopp[b], P. Chiba[b] and G.F. Ecker*[,a]

[a]*Department of Pharmaceutical Chemistry, University of Vienna, Althanstrasse 14, 1090 Wien, Austria;* [b]*Institute of Medical Chemistry, Medical University of Vienna, Waehringerstrasse 10, 1090 Wien, Austria*

Abstract: Overexpression of membrane bound, ATP-dependent transport proteins is one of the predominant mechanisms leading to multiple drug resistance in tumor therapy as well as in the treatment of bacterial and fungal infections. In tumor therapy, P-glycoprotein (P-gp, ABCB1) is responsible for transport of a wide variety of natural product toxins out of tumor cells leading to decreased accumulation of cytotoxic drugs within the cells. Inhibition of P-gp thus gives rise to a resensitization of multidrug resistant tumor cells and represents a versatile approach for modulation of multidrug resistance.

Within this paper, a set of propafenone-type inhibitors of P-gp were analyzed using both interaction field based methods such as CoMFA and CoMSIA and Hologram QSAR. With both methods, highly predictive models with q^2-values > 0.65 were obtained. Models using logP as additional descriptor generally yielded higher predictive power. On basis of unfavorable steric and favorable electrostatic and hydrophobic interaction fields, these models were able to explain all outlayers identified in previous Hansch-analyses.

For HQSAR analysis, models with q^2-values up to 0.72 were obtained. Positive influences were found for electron donating groups on the aromatic systems. Highly negative influences were found for diphenylalkylamine substituents, which is a further hint for steric hindrance. The models with highest predictive power were used for screening of a small virtual library. Synthesis and pharmacological testing of a sub set of this library showed that the external predictivity of the HQSAR models generally is lower than the internal one.

Key Words: P-glycoprotein, multidrug resistance, CoMFA, CoMSIA, hologram QSAR, propafenone, virtual screening.

INTRODUCTION

Drug efflux pumps have been shown to represent challenging targets for medicinal chemists. These membrane bound, energy driven transport proteins recognize a wide variety of structurally and functionally diverse drugs and hinder them to enter the cell [1]. Substrates include many anticancer [2], antifungal [3], antibacterial [4] and antiprotozoal drugs [5] which makes these proteins a serious impediment in the chemotherapy of cancer and infectious diseases. In humans, 48 so called ABC (ATP-binding casette) transporters have been identified so far, a number of which have been linked to drug transport processes [6]. However, some of these are also expressed at the blood-brain barrier and protect the brain from entrance of toxic compounds [7]. Thus, these proteins also play an important physiological role [8].

In the Medicinal Chemistry field, research focused predominantly on P-glycoprotein (P-gp, ABCB1) and inhibitors thereof [9]. P-gp is overexpressed in a wide variety of tumors and was linked to multiple drug resistance. Inhibitors of P-gp thus represent a versatile tool for overcoming resistance and resensitizing multidrug resistant tumors. Several compounds have reached phase III clinical studies [10]. However, results are not as promising as expected and the general therapeutic applicability of P-gp inhibitors to overcome multiple drug resistance is still unclear. Within the past few years, research on substrates of P-gp gained increasing interest. Due to the expression of P-gp in the gastrointestinal mucosa as well as in the blood-brain barrier its role in the ADME process became a major focus in pharmaceutical research [11]. Recently several compounds were claimed, which increase bioavailability and brain uptake of drugs *via* inhibition of P-gp [12]. In the field of CNS-research, poor brain uptake of compounds is increasingly related to their P-gp substrate properties [13].

Although numerous QSAR-studies on P-gp ligands have been performed on different compound series [14], only a few used 3D-QSAR methods to gain informations on the three-dimensional requirements for compounds interacting with P-gp. Pajeva and Wiese performed CoMFA and CoMSIA analyses on a small set of propafenones [15] and phenothiazines [16]. The group of Ekins reported three-dimensional pharmacophore models based on *in vitro* data for digoxin transport in Caco-2 cells, vinblastine binding in CEM/VLB_{100} cells and vinblastine and calcein accumulation in LLC-PK1 cells [17]. Additionally, definition of pharmacophores and alignment was utilized using the genetic algorithm based similarity program GASP. The proposed

*Address correspondence to this author at the Department of Pharmaceutical Chemistry, University of Vienna, Althanstrasse 14, 1090 Wien, Austria; Tel: +43-1-4277-55110; Fax: +43-1-4277-9551; E-mail: gerhard.f.ecker@univie.ac.at

1573-4064/05 $50.00+.00

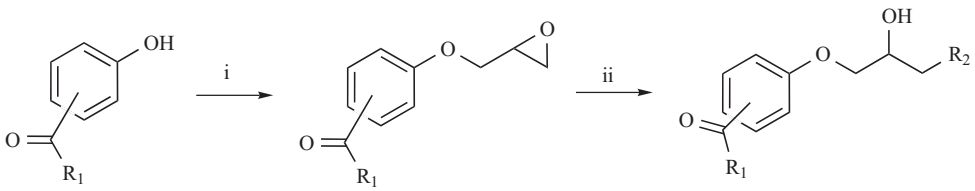

Scheme (1). General scheme for synthesis of propafenones; i epichlorohydrine; ii amine.

Table 1. Chemical Structure and PGP-inhibitory Activity (in μM) of Propafenone Derivatives; GPV Codes Refer to Compounds of the Training Set, DKD Codes to Those of the Virtual Library

Code	Core	R1 - R4	L	A	EC_{50} (μM)
GPV 0001	A	R1 = $COCH_2CH_2Ph$	$-CH_2CH(OH)CH_2-$	–NH(*n*Pr)	0.329
GPV 0002	A	R1 = $COCH_2CH_2Ph$	$-CH_2CH(OH)CH_2-$	$-N(C_2H_5)_2$	0.907
GPV 0005	A	R1 = $COCH_2CH_2Ph$	$-CH_2CH(OH)CH_2-$	A1	0.599
GPV 0009	A	R1 = $COCH_2CH_2Ph$	$-CH_2CH(OH)CH_2-$	$-N(iPr)_2$	0.377
GPV 0012	A	R1 = $COCH_2CH_3$	$-CH_2CH(OH)CH_2-$	A1	14.31
GPV 0017	A	R1 = $COCH_3$	$-CH_2CH(OH)CH_2-$	A1	31.96
GPV 0019	A	R1 = $COCH_2CH_2Ph$	$-CH_2CH(OH)CH_2-$	A3	0.610
GPV 0021	A	R1 = $COCH_2CH_2Ph$	$-CH_2CH(OH)CH_2-$	A4	0.230
GPV 0023	A	R1 = $COCH_2CH_2Ph$	$-CH_2CH(OH)CH_2-$	A5	0.678
GPV 0025	A	R1 = $COCH_2CH_2Ph$	$-CH_2CH(OH)CH_2-$	A6	0.256
GPV 0027	A	R1 = $COCH_2CH_2Ph$	$-CH_2CH(OH)CH_2-$	A7	0.027
GPV 0029	A	R1 = $COCH_2CH_2Ph$	$-CH_2CH(OH)CH_2-$	A10	0.659
GPV 0031	A	R1 = $COCH_2CH_2Ph$	$-CH_2CH(OH)CH_2-$	A8	0.070
GPV 0045	A	R1 = $COCH_3$	$-CH_2CH(OH)CH_2-$	A8	2.087
GPV 0046	A	R1 = $COCH_2CH_3$	$-CH_2CH(OH)CH_2-$	A2	207.2
GPV 0048	A	R1 = $COCH_2CH_2Ph$	$-CH_2CH(OH)CH_2-$	$-N(CH_3)_2$	2.479
GPV 0049	A	R1 = $COCH_3$	$-CH_2CH(OH)CH_2-$	A2	67.32
GPV 0050	A	R1 = $COCH_2CH_2Ph$	$-CH_2CH(OH)CH_2-$	$-N(CH_3)nPr$	0.416
GPV 0051	A	R1 = COPh	$-CH_2CH(OH)CH_2-$	$-N(C_2H_5)_2$	2.322
GPV 0057	A	R1 = $COCH_2CH_2Ph$	$-CH_2CH(OH)CH_2-$	A2	3.645
GPV 0062	A	R1 = $COCH_2CH_2Ph$	$-CH_2CH(OH)CH_2-$	A12	0.058
GPV 0073	A	R3 = $COCH_2CH_2Ph$	$-CH_2CH(OH)CH_2-$	A1	0.972
GPV 0088	A	R1 = $CH(OH)CH_2CH_2Ph$	$-CH_2CH(OH)CH_2-$	A1	0.901
GPV 0090	A	R1 = $CH(OCH_3)CH_2CH_2Ph$	$-CH_2CH(OH)CH_2-$	A1	0.173
GPV 0091	B	R1 = CH_2CH_2Ph	$-(CH_2)_2-$	A1	0.980
GPV 0092	B	R1 = CH_2CH_3	$-CH(OH)CH_2-$	–NH(*n*Pr)	11.52
GPV 0093	B	R1 = CH_2CH_2Ph	(S) $-CH(OH)CH_2-$	–NH(*n*Pr)	1.059
GPV 0094	B	R1 = CH_2CH_2Ph	(R) $-CH(OH)CH_2-$	–NH(*n*Pr)	1.103
GPV 0095	B	R1 = CH_2CH_2Ph	$-CH(OH)CH_2-$	A4	0.177

(Table 1. Contd….)

Code	Core	R1 - R4	L	A	EC_{50} (μM)
GPV 0128	A	R1 = $COCH_2CH_2Ph$	$-CH_2CH(OH)CH_2-$	A11	0.259
GPV 0129	A	R1 = $COCH_2CH_2Ph$, R3 = OH	$-CH_2CH(OH)CH_2-$	–NH(*n*Pr)	3.021
GPV 0134	A	R3 = $COCH_2CH_2Ph$	$-CH_2CH(OH)CH_2-$	A8	2.535
GPV 0135	A	R2 = $COCH_2CH_2Ph$	$-CH_2CH(OH)CH_2-$	A1	0.424
GPV 0149	A	R3 = $COCH_2CH_2Ph$	$-CH_2CH(OH)CH_2-$	A2	6.875
GPV 0155	A	R1 = $CH(OH)CH_2CH_2Ph$	$-CH_2CH(OH)CH_2-$	A8	0.671
GPV 0156	A	R1 = $CH(OCH_3)CH_2CH_2Ph$	$-CH_2CH(OH)CH_2-$	A8	0.226
GPV 0157	A	R2 = $COCH_2CH_2Ph$	$-CH_2CH(OH)CH_2-$	A8	1.120
GPV 0159	A	R3 = $COCH_2CH_2Ph$	$-CH_2CH(OH)CH_2-$	$-N(iPr)_2$	0.915
GPV 0163	A	R1 = $CH(OH)CH_2CH_2Ph$	$-CH_2CH(OH)CH_2-$	$-N(iPr)_2$	1.741
GPV 0164	A	R1 = $CH(OCH_3)CH_2CH_2Ph$	$-CH_2CH(OH)CH_2-$	$-N(iPr)_2$	0.658
GPV 0180	A	R1 = $COCH_2CH_2$-(1-naphthyl)	$-CH_2CH(OH)CH_2-$	A1	0.172
GPV 0181	A	R1 = $COCH_2CH_2Ph$	$-CH_2CH(OH)CH_2-$	$-NH(CH_2CH(Ph)_2)$	0.797
GPV 0182	A	R1 = $COCH_2CH_2Ph$	$-CH_2CH(OH)CH_2-$	$-NH(CH(Ph)_2)_2$	10.40
GPV 0184	A	R1 = $COCH_2CH_2$-(1-naphthyl)	$-CH_2CH(OH)CH_2-$	$-NH(CH_2CH_2CH(Ph)_2)$	0.723
GPV 0186	A	R1 = $COCH_2CH_2Ph$	$-(CH_2)_3-$	A1	0.651
GPV 0189	A	R1 = $COCH_2CH_2Ph$	$-(CH_2)_2-$	A1	1.452
GPV 0195	A	R1 = $COCH_2CH_2Ph$	$-(CH_2)_4-$	A1	0.533
GPV 0201	A	R1 = $COCH_2CH_2Ph$	$-(CH_2)_5-$	A1	0.242
GPV 0206	A	R1 = $COCH_2CH_2Ph$	$-(CH_2)_6-$	A1	0.203
GPV 0211	A	R1 = $COCH_2CH_2Ph$	$-(CH_2)_7-$	A1	0.179
GPV 0216	A	R1 = $COCH_2CH_2Ph$	$-(CH_2)_8-$	A1	0.137
GPV 0220	A	R1 = $CH(OCH_3)CH_2CH_2Ph$	$-CH_2CH(OH)CH_2-$	$-NH(CH_2CH_2CH(Ph)_2)$	0.752
GPV 0226	A	R1 = $CH(OH)CH_2CH_2Ph$	$-CH_2CH(OH)CH_2-$	A2	9.540
GPV 0227	A	R1 = $CH(OCH_3)CH_2CH_2Ph$	$-CH_2CH(OH)CH_2-$	A2	1.807
GPV 0231	A	R1 = $COCH_2CH_2Ph$, R3 = OBz	$-CH_2CH(OH)CH_2-$	–NH(*n*Pr)	0.110
GPV 0232	A	R1 = $COCH_2CH_2Ph$, R3 = OBz	$-CH_2CH(OH)CH_2-$	A1	0.172
GPV 0233	A	R1 = $COCH_2CH_2Ph$, R3 = OH	$-CH_2CH(OH)CH_2-$	A1	1.727
GPV 0238	A	R1 = $COCH_2CH_2Ph$	$-CH_2CH(OH)CH_2-$	$-NH(CH_2CH_2CH(Ph)_2)$	0.717
GPV 0240	A	R1 = $COCH_2CH_2Ph$	$-CH_2CH(OH)CH_2-$	–NH(Ph)	6.467
GPV 0242	A	R1 = $COCH_2CH_2Ph$	$-CH_2CH(OH)CH_2-$	–NH(cyclohexyl)	0.341
GPV 0245	A	R1 = $COCH_2CH_2Ph$, R3 = OH	$-CH_2CH(OH)CH_2-$	$-N(iPr)_2$	1.036
GPV 0253	A	R1 = $COCH_2CH_2Ph$, R3 = OBz	$-CH_2CH(OH)CH_2-$	A10	0.116
GPV 0264	A	R1 = $CH(iPr)CH_2CH_2Ph$	$-CH_2CH(OH)CH_2-$	A1	0.460
GPV 0317	A	R1 = COPh	$-CH_2CH(OH)CH_2-$	A12	0.307
GPV 0319	A	R1 = COPh	$-CH_2CH(OH)CH_2-$	A8	0.147

(Table 1. Contd….)

Code	Core	R1 - R4	L	A	EC_{50} (μM)
GPV 0321	A	R1 = $COCH_3$	–$CH_2CH(OH)CH_2$–	A11	0.357
GPV 0323	A	R1 = $COCH_3$	–$CH_2CH(OH)CH_2$–	A12	3.197
GPV 0334	A	R1 = $COCH_2CH_2$(4-Cl-Ph)	–$CH_2CH(OH)CH_2$–	A7	0.019
GPV 0335	A	R1 = $COCH_2CH_2$(4-CH_3-Ph)	–$CH_2CH(OH)CH_2$–	A7	0.018
GPV 0336	A	R1 = $COCH_2CH_2$(4-OCH_3-Ph)	–$CH_2CH(OH)CH_2$–	A7	0.014
GPV 0338	A	R1 = $COCH_2CH_2Ph$	–$CH_2CH(OAc)CH_2$–	A1	0.336
GPV 0339	A	R1 = $COCH_2CH_2Ph$	–$CH_2CH(OH)CH_2$–	–NH(Ph-4-$COOCH_3$)	1.536
GPV 0354	A	R1 = $COCH_2CH_2Ph$, R3 = Cl	–$CH_2CH(OH)CH_2$–	A7	0.059
GPV 0356	A	R1 = $COCH_2CH_2Ph$, R3 = OCH_3	–$CH_2CH(OH)CH_2$–	A7	0.179
GPV 0357	A	R1 = $COCH_2CH_2Ph$, R3 = CH_3	–$CH_2CH(OH)CH_2$–	A7	0.026
GPV 0358	A	R1 = $COCH_2CH_2Ph$	–$CH_2CH(OH)CH_2$–	–NH(Ph-4-CF_3)	8.490
GPV 0359	A	R1 = $COCH_2CH_2Ph$	–$CH_2CH(OH)CH_2$–	–NH(Ph-4-NO_2)	2.568
GPV 0360	A	R1 = $COCH_2CH_2Ph$	–$CH_2CH(OH)CH_2$–	–N($COCH_2CH_3$)Bz	1.649
GPV 0361	A	R1 = $COCH_2CH_2Ph$	–$(CH_2)_4$–	A2	1.006
GPV 0363	A	R1 = $COCH_2CH_2Ph$	–$(CH_2)_4$–	A8	0.192
GPV 0366	A	R1 = $COCH_2CH_2Ph$	–$CH_2CH(OH)CH_2$–	–N(*n*Pr)COPh	1.686
GPV 0374	A	R1 = $COCH_2CH_2$-(1-naphthyl)	–$CH_2CH(OH)CH_2$–	A2	0.730
GPV 0376	A	R1 = $COCH_2CH_2$-(1-naphthyl)	–$CH_2CH(OH)CH_2$–	–N(*i*Pr)$_2$	0.465
GPV 0381	A	R1 = $COCH_2CH_3$	–$CH_2CH(OH)CH_2$–	A12	0.299
GPV 0382	A	R1 = $COCH_2CH_2$-(1-naphthyl)	–$CH_2CH(OH)CH_2$–	A12	0.075
GPV 0384	A	R2 = $COCH_3$	–$CH_2CH(OH)CH_2$–	A2	128.4
GPV 0385	A	R2 = $COCH_3$	–$CH_2CH(OH)CH_2$–	A1	9.073
GPV 0386	A	R2 = $COCH_3$	–$CH_2CH(OH)CH_2$–	A8	10.07
GPV 0388	A	R1 = $COCH_2CH_2Ph$	–$CH_2CH(OH)CH_2$–	A13	0.130
GPV 0389	A	R3 = $COCH_3$	–$CH_2CH(OH)CH_2$–	A1	48.97
GPV 0390	A	R3 = $COCH_3$	–$CH_2CH(OH)CH_2$–	A8	11.89
GPV 0391	A	R3 = $COCH_3$	–$CH_2CH(OH)CH_2$–	A2	302.1
GPV 0476	A	R1 = $COCH_2CH_2Ph$, R3 = Cl, R4 = Cl	–$CH_2CH(OH)CH_2$–	A7	0.017
GPV 0479	A	R1 = $COCH_3$, R3 = CH_3	–$CH_2CH(OH)CH_2$–	A1	5.470
GPV 0485	C	R1 = H, R2 = O, R3 = H,H	–$CH_2CH(OH)CH_2$–	A1	9.684
GPV 0512	C	R1 = H, R2 = H,H, R3 = O	–$CH_2CH(OH)CH_2$–	A1	11.19
GPV 0570	A	R1 = $COCH_2CH_2Ph$	–CH_2COOEt	---------	23.18
GPV 0574	A	R3 = $COCH_3$	–$CH_2CH(OH)CH_2$–	A9	1.349
GPV 0576	A	R1 = $COCH_2CH_2Ph$	–$CH_2CH(OH)CH_2$–	A9	0.006
GPV 0577	A	R3 = $COCH_3$	–$CH_2CH(OH)CH_2$–	A7	1.550
GPV 0579	A	R2 = $COCH_3$	–$CH_2CH(OH)CH_2$–	A9	0.379

(Table 1. Contd….)

Code	Core	R1 - R4	L	A	EC_{50} (μM)
GPV 0596	A	R2 = $COCH_3$	–$CH_2CH(OH)CH_2$–	A7	0.537
GPV 0598	A	R1 = $COCH_3$	–$CH_2CH(OH)CH_2$–	A9	0.200
GPV 0600	A	R3 = $COCH_2CH_2Ph$	–$CH_2CH(OH)CH_2$–	A9	0.227
GPV 0608	A	R1 = $COCH_2CH_2Ph$, R4 = OCH_3	–$CH_2CH(OH)CH_2$–	A7	0.296
GPV 0610	A	R1 = $COCH_2CH_2$-(4-$N(CH_3)_2$-Ph)	–$CH_2CH(OH)CH_2$–	A7	0.013
GPV 0613	A	R1 = $COCH_3$, R3 = OCH_3	–$CH_2CH(OH)CH_2$–	A7	0.859
GPV 0615	A	R1 = $COCH_3$, R3 = CH_3	–$CH_2CH(OH)CH_2$–	A7	0.396
GPV 0616	A	R1 = $COCH_3$, R3 = $COCH_3$, R4 = CH_3	–$CH_2CH(OH)CH_2$–	A7	0.211
GPV 0626	A	R1 = $COCH_3$	–$CH_2CH(OH)CH_2$–	A7	0.249
GPV 0633	A	R1 = $COCH_3$, R4 = CH_3	–$CH_2CH(OH)CH_2$–	A7	0.162
GPV 0636	A	R1 = COCH3, R3 = Cl, R4 = Cl	–$CH_2CH(OH)CH_2$–	A7	0.125
GPV 0643	A	R1 = $COCH_2CH_2$-(4-$N(CH_3)_2$-Ph), R4 = OCH_3	–$CH_2CH(OH)CH_2$–	A7	0.040
GPV 0645	A	R3 = $COCH_3$	–$CH_2CH(OH)CH_2$–	–$NH(CH_2CH_2CH(Ph_2))$	0.178
GPV 0647	A	R2 = $COCH_2CH_2Ph$	–$CH_2CH(OH)CH_2$–	A7	0.074
GPV 0649	A	R2 = $COCH_2CH_2Ph$	–$CH_2CH(OH)CH_2$–	–$NH(CH_2CH_2CH(Ph_2))$	0.190
GPV 0651	A	R2 = $COCH_2CH_2Ph$	–$CH_2CH(OH)CH_2$–	A9	0.137
GPV 0653	A	R2 = $COCH_2CH_2Ph$	–$CH_2CH(OH)CH_2$–	A2	3.475
GPV 0655	A	R3 = $COCH_2CH_2Ph$	–$CH_2CH(OH)CH_2$–	–$NH(CH_2CH_2CH(Ph_2))$	0.505
DKD 001	A	R1 = $CH(OH)CH_2CH_2Ph$	–$CH_2CH(OH)CH_2$–	A10	0.188
DKD 004	A	R1 = $CH(OCH_3)CH_2CH_2Ph$	–$CH_2CH(OH)CH_2$–	A10	0.080
DKD 006	A	R1 = $COCH_3$	–$CH_2CH(OH)CH_2$–	–$N(i\text{Pr})_2$	10.09
DKD 013	A	R1 = $COCH_2CH_3$	–$CH_2CH(OH)CH_2$–	A8	0.836
DKD 014	A	R1 = $COCH_2CH_3$	–$CH_2CH(OH)CH_2$–	–$N(i\text{Pr})_2$	4.285
DKD 015	A	R1 = $COCH_2CH_3$	–$CH_2CH(OH)CH_2$–	A10	1.445
DKD 016	A	R1 = $COCH_2CH_3$	–$CH_2CH(OH)CH_2$–	–$NH(CH_2CH_2CH(Ph_2))$	0.121
DKD 024	A	R3 = $COCH_2CH_2Ph$	–$CH_2CH(OH)CH_2$–	–$NH(CH_2CH_2CH(Ph_2))$	0.505
DKD 032	A	R1 = $COCH_2CH_2Ph$, R3 = OCH_2Ph	–$CH_2CH(OH)CH_2$–	A12	0.086
DKD 037	A	R3 = $COCH_3$	–$CH_2CH(OH)CH_2$–	–$NH(CH_2CH_2CH(Ph_2))$	0.178
DKD 039	A	R2 = $COCH_2CH_2Ph$	–$CH_2CH(OH)CH_2$–	A2	3.475
DKD 042	A	R2 = $COCH_2CH_2Ph$	–$CH_2CH(OH)CH_2$–	–$NH(CH_2CH_2CH(Ph_2))$	0.190

general pharmacophore pattern involves two hydrophobic points, three hydrogen bond acceptors (HBA) and one hydrogen bond donor (HBD) [18]. Very recently we demonstrated, that a chemical function based pharmacophoric feature model based on 15 propafenone-type inhibitors is suitable for *in silico* screening of compound libraries [19]. However, applying these models for virtual screening approaches requires multi-conformational three-dimensional databases. Within this study we performed both a CoMFA and CoMSIA study on an extended set of propafenone-type P-gp inhibitors and for the first time in this field also explored the holographic QSAR method for model generation and virtual library screening.

MATERIALS AND METHODS

Chemistry

Compounds were prepared analogous to previously described procedures [19-21]. Briefly, an appropriate phenol

(1) was O-alkylated with epichlorohydrine. Reaction of the resulting epoxides with the corresponding amines lead to the target compounds (Scheme 1). Phenols were synthesized *via* aldol condensation of hydroxyacetophenone derivatives with the appropriate aldehyde and subsequent catalytic hydrogenation. The chemical structure, physicochemical parameters and biological activity are given in Table **1**. The corresponding core structures A-C and amine moieties A1-A13 are shown in Fig. (**1**).

CoMFA and CoMSIA Studies

IC_{50}-values reported in this paper correspond to racemic mixtures. Previous SAR studies of pure enantiomers of propafenone showed small, but statistically significant differences with the R-isomer being the more potent one [22]. Therefore, in the CoMFA and CoMSIA studies the asymmetric carbon atom of the aminopropan-2-ol fragment was modeled with R-configuration. A similar study of 1-phenylpropan-1-ol analogues showed almost no differences

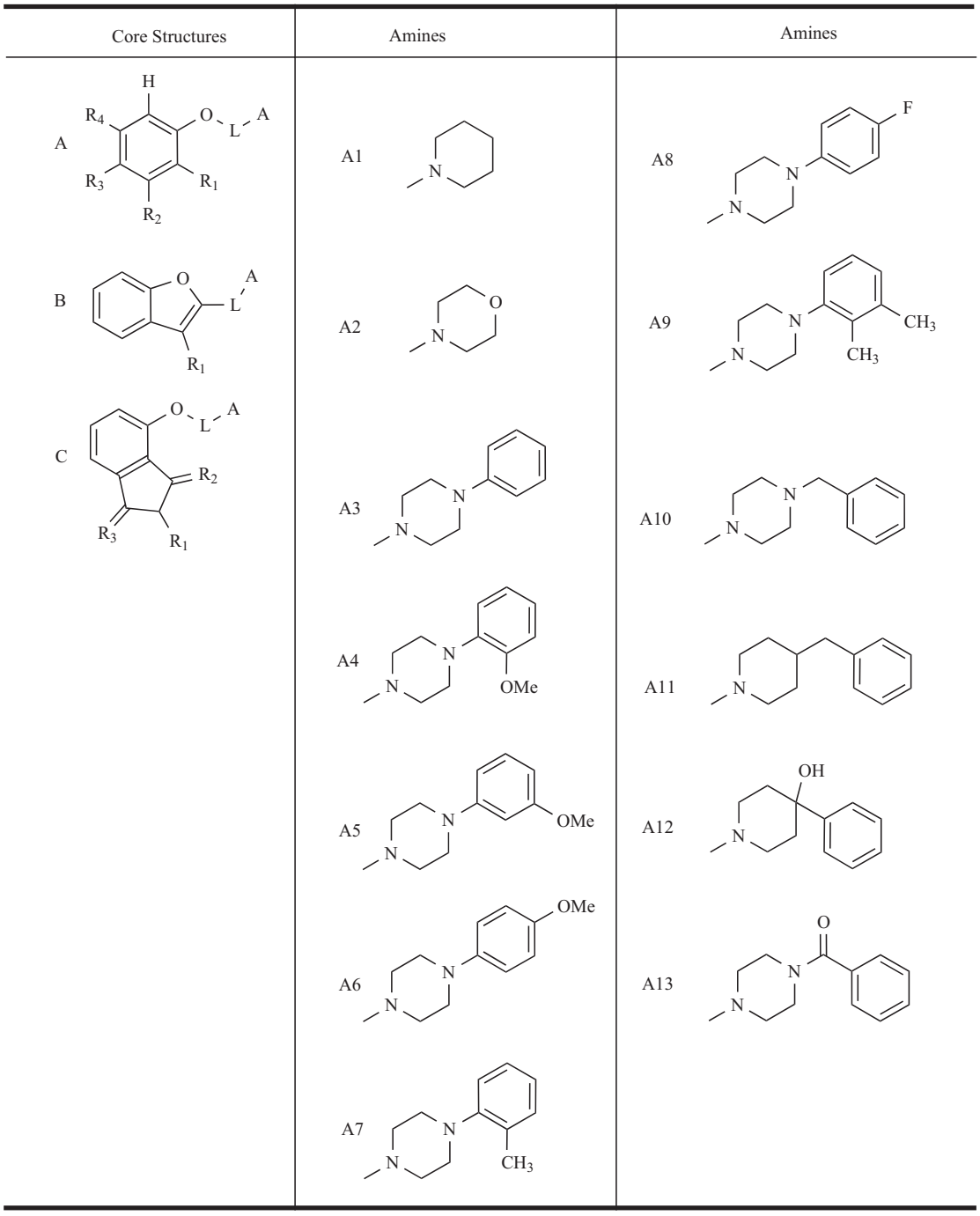

Fig. (1). Core structures of propafenone derivatives.

between the stereoisomers. In this case (GPV 0088, GPV 0090 and analogues) the asymmetric benzylic carbon atom was modeled with R-configuration.

Although several authors stressed the importance of a positively ionizable nitrogen atom, only the neutral forms of the molecules were considered. This is in accordance with our previous findings, that the basic nitrogen atom interacts due to its H-bond acceptor strength rather than its basicity [23].

Currently no crystal structure is available for any of the compounds studied. Thus, the starting geometry of each compound was obtained using the 3D-structure generator CORINA [24]. Conformations obtained are in agreement with those used by Pajeva [15], thus orienting the carbonyl oxygen in ortho-substituted derivatives atom towards the ether oxygen. However, in a substructure search in the Cambridge Crystallographic Database [25] two structures were found: acebutolol (refcode ACBUOL) and celiprolol (refcode KUDVEK). Both compounds contain a 2-(3-amino-2-hydroxypropoxy)-acetophenone substructure with the carbonyl oxygen oriented outwards and away from the ether oxygen (dihedral angle values –167.1° and –166.0°; Fig. (**2**). Additionally, also the pharmacophore hypothesis obtained previously for a set of propafenone analogues shows this arrangement with the H-bond acceptor feature pointing outwards [19]. The appropriate dihedral angles were thus set according to the values found for celiprolol. Subsequent geometry optimization and calculation of Coulson charges were performed with the MOPAC module of SYBYL 6.5 [26] using the semiempirical AM1 method with full optimization, normal convergence, precise criteria and net charge 0.

The most active compound GPV 0576 was selected as template. For the structure alignment the aromatic ring centroids A, B, and C were created (Fig. (**2**). Previous QSAR studies showed, that both aromatic rings of the propiophenone-moiety, the carbonyl oxygen atom, the amine nitrogen atom and a hydrophobic group on the nitrogen atom are beneficial for high pharmacological activity. Corresponding features were also found in the pharmacophoric feature modeling approach. Thus, if not otherwise stated, these 5 points were used in the alignment for pairwise fitting (rms fit) of all structures. In compounds GPV 0180, GPV 0184, GPV 0374 and GPV 0376 the centroid B represents the whole naphthalene ring. Compounds GPV 0073, GPV 0092, GPV 0149, GPV 0574 and GPV 0577 did not contain the minimum of three common points needed for alignment. for these compounds the hydroxyl oxygen atom of the aminopropan-2-ol fragment was used as additional pair together with ring A and the amine nitrogen atom. Phenyl ring B of benzophenones GPV 0051, GPV 0317 and GPV 0319 was not aligned to phenyl ring B of GPV 0576 as this distorts the alignment pattern. The carbonyl oxygen atom of meta-substituted analogues was used for alignment of these compounds. Due to a different steric location the carbonyl oxygen atom of para-substituted compounds was not used for alignment. Similarly, the phenyl ring B of both meta- and para-substituted compounds was not aligned to the ring B of template GPV 0576. The piperidine nitrogen atom of compounds GPV 0201, GPV 0206, GPV 0211 and GPV 0216 was aligned to the aniline-type nitrogen atom in template GPV 0576. Fig. (**3**) shows an overlay of all 119 compounds aligned according to the above outlined criteria.

All possible combinations of calculated fields, logP and IC_{50} values were examined by PLS leave-one-out cross-validation procedure. Cross-validated Q^2 values and optimal number of components N_{opt} were recorded for each run. Next, the r^2 and standard error of estimation (SEE) were calculated for the best model found in the cross validation runs.

HQSAR Studies

Molecular holograms are related to 2D fingerprinting. Given an input molecule, all possible structural fragments –

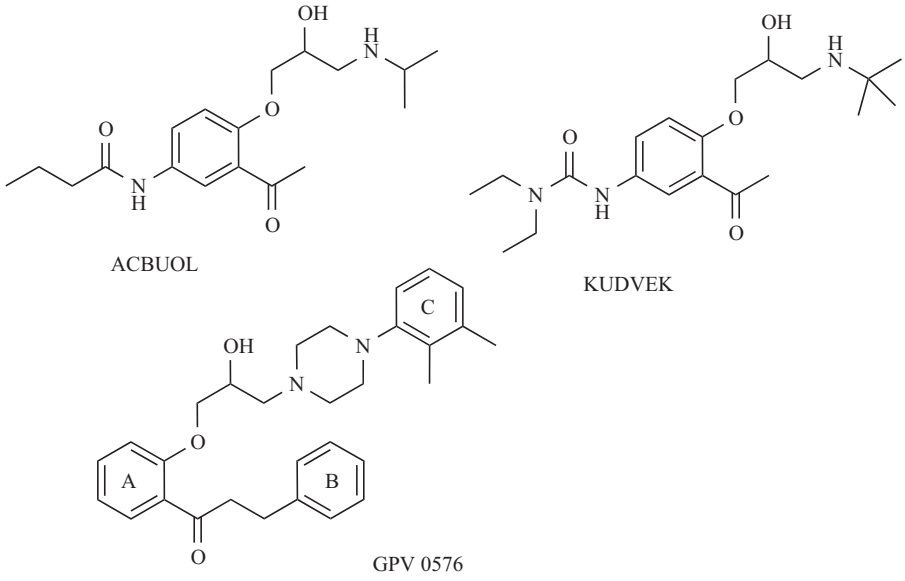

Fig. (2). chemical structures of acebutolol, celiprolol and GPV 0576.

Fig. (3). Alignment of 119 propafenones used for 3D-QSAR studies.

including overlapping fragments – that contain a user-defined minimum and maximum number of atoms are generated. Subsequently, unique identifiers are assigned to each of the resulting types of fragments and these integer identifiers are hashed into an L-integer array of a user defined length to give the molecular hologram. This array is subsequently used in PLS analyses [27]. For our study models with all possible combinations of atoms (A), bonds (B), connections (C), hydrogen atoms (H) and donor & acceptor (D) were generated. Hologram lengths of 353, 307, 257, 199, 151, 97, 83, 71, 61, 59, 53, 43, 41, 37, 31, 29 and 23 were used. The maximum number of components was set to 10 and the minimum and maximum fragment length was set to 4 and 7, respectively.

Pharmacological Activity

The human T-lymphoblast cell line CCRF-CEM and the multidrug resistant line CCRF VCR1000 were provided by V. Gekeler (Byk Gulden, Konstanz, Germany). The resistant line was obtained by stepwise selection in vincristine containing medium [28]. Cells were kept under standard culture conditions (RPMI 1640 medium supplemented with 10% fetal calf serum). The Pgp-expressing resistant cell line was cultured in presence of 1000ng/ml vincristine. One week prior to the experiments cells were transferred into medium without selective agents or antibiotics.

Daunorubicine efflux studies were performed as described [29]. Briefly, cells were pelleted, the supernatant was removed by aspiration and cells were resuspended at a density of 1 x 10^6/ml in PRMI1640 medium containing 3µmol/l daunorubicine. Cell suspensions were incubated at 37°C for 30min. After this time a steady state of daunorubicine accumulation was reached. Tubes were chilled on ice and cells were pelleted at 500 x g. Cells were washed once in RPMI1640 medium to remove extracellular daunorubicine. Subsequently, cells were resuspended in medium prewarmed to 37°C, containing either no modulator or chemosensitiser at various concentrations ranging from 3nM to 500 µM, depending on solubility and expected potency of the modifier. Generally, 8 serial dilutions were tested for each modulator. After 1, 2, 3 and 4 min aliquots of the incubation mixture were drawn and pipetted into 4 volumes of ice cold stop solution (RPMI1640 medium containing verapamil at a final concentration of 100µM). Parental CCRF-CEM cells were used to correct for simple membrane diffusion, which was less than 3% of the efflux rate observed in resistant cells. Samples drawn at the respective time points were kept in an ice water bath and measured within an hour in a Becton Dickonson FACSCalibur flow cytometer. Dose response curves were fitted to the data points using non-linear least squares and EC_{50} values were calculated.

RESULTS AND DISCUSSION

Propafenone and its analogs have been shown to be potent inhibitors of P-glycoprotein and thus represent a versatile tool for exploring structure-activity relationship studies on this drug efflux pump [30]. The aryloxypropanol-amine scaffold exhibits several pharmacophoric sub-structures as identified by Klopman [31] and offers a broad structural variability utilizing only 3-5 synthetic steps. Systematic Hansch analyses combined with a Free-Wilson approach gave distinct informations on the SAR within this compound class (reviewed in [30]). However, these studies only rely on the 2D-structure of the molecules. To further extend our studies, we used also 3D-QSAR methods, which should complement our protein homology modeling attempts. Additionally, we applied the recently developed hologram QSAR methodology to our propafenone data set.

3D-QSAR Studies

In 3D-QSAR studies the conformation of the molecules and in case of CoMFA and CoMSIA also the alignment of the compounds are crucial steps to be performed. Although there is no X-ray structure of propafenone available, two structurally analogous o-acylphenyloxypropanolamines were

found in the Cambridge database (acebutolol and celiprolol). Both compounds show the carbonyl group poiting outwards and away from the ether oxygen atom of the molecule. This is in contrast to the conformations used by Pajeva and Wiese for a CoMFA study performed recently on a small subset of our series and also does not reflect the orientation obtained by CORINA. However, our very recently published pharmacophoric feature model of propafenone-type P-gp inhibitors also supports a more outward orientation of the carbonyl group, which enables H-bonds to be formed with the protein. This is also supported by our Hansch-analyses, which outlined the importance of the carbonyl group with regard to its H-bond acceptor properties [32]. Thus, the appropriate dihedral angles were set according to the values found in celiprolol. For the alignment, the most active compound GPV 0576 was selected as template. According to the results of our previously performed QSAR-studies, both aromatic rings of the propiophenone-moiety, the carbonyl oxygen atom, the amine nitrogen atom and a hydrophobic group on the nitrogen atom were used in the alignment. Corresponding features were also found in the pharmacophoric feature modeling approach. Thus, these 5 points were used in the alignment for pairwise fitting (rms fit) of all structures, if not otherwise stated in the methods section.

The 3D-QSAR models derived from the training set of 119 compounds are presented in Tables **2** (CoMFA) and 3 (CoMSIA).

Models were calculated for each field alone and in combination with other fields to investigate the influence of a given molecular property. Additionally, due to the general importance of lipophilicity as predictive factor, we also included calculated logP values as descriptor. In case of CoMFA, this generally gave higher internal predictivity than CoMFA fields alone. This further strengthens the beneficial influence of high lipophilicity on P-gp inhibitory activity. The highest Q^2 value was obtained with the model including both steric and electrostatic interaction fields as well as H-bond and logP values (Figure 4).

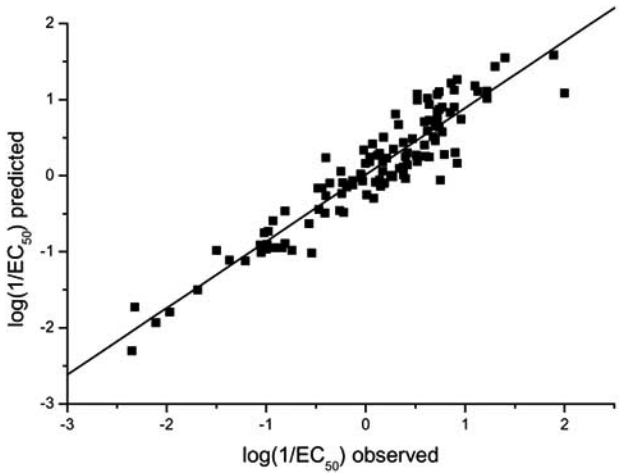

Fig. (4). Plot of observed *vs*. predicted (leave one out cross validation) $\log(1/EC_{50})$ values for the CoMFA model.

When analyzing the contour plots (Figures 5a and 5b), the following main conclusions can be drawn:

-) An important unfavorable steric interaction is observed in compounds with bulky substituents (e.g. diphenylmethyl) on the aminopropanol nitrogen atom.

Table 2. CoMFA Models Derived from 119 Propafenone-type P-gp Inhibitors

Model	Q^2	N_{opt}	r^2	SEE
Steric	0.635	11	0.935	0.216
Electrostatic	0.481	5	0.807	0.364
Both	**0.650**	**5**	**0.877**	**0.291**
Steric + H-Bond	0.645	4	0.827	0.343
Electrostatic + H-Bond	0.572	5	0.840	0.331
Both + H-Bond	0.630	4	0.835	0.335
H-Bond	0.253	4	0.626	0.504
Steric + logP	0.627	4	0.776	0.391
Electrostatic + logP	0.603	3	0.752	0.409
Both + logP	0.669	4	0.815	0.355
Steric + H-Bond + logP	0.679	4	0.836	0.334
Electrostatic + H-bond + logP	0.662	4	0.834	0.336
Both + H-Bond + logP	**0.692**	**4**	**0.849**	**0.320**
H-Bond + logP	0.634	4	0.797	0.371

-) A favorable steric interaction is observed in the region of phenyl ring B, i.e. more bulky substituents should improve activity.

-) With regard to favorable electrostatic interactions, both the carbonyl oxygen and the propanolamine nitrogen atom are important for high activity. However, as shown recently, this interactions seems to be correlated to the H-bond acceptor strength of this area rather than an electrostatic interaction [23].

In comparison to the models obtained by Pajeva and Wiese, the Q^2 values obtained in our study are generally lower. This seems to be mainly due to the limited data set available at the time when the previous CoMFA study was performed (28 compounds). In principle, this set contained propafenones, the corresponding hydroxy and methoxy-analogs, 2 meta- and para-acyl derivatives and structurally constrained benzofuranes. Using calculated logP values and three indicator variables (for benzofuranes, non-phenones and meta- or para-substitution on the central aromatic ring) for multiple linear regression analysis gives already a correlation with an r^2 value of 0.68. The extended set used in this study includes also several compounds which showed clear outlier characteristics in the overall logP/log potency relationship. These include the hydroxyphenylpiperidines GPV 0062, 0317, 0323, 0381, 0382, diphenylalkylamines GPV 0181, 0182, 0184, 0220, 0238, 0645, 0649, 0655, as well as anilines GPV 0339, 0358, 0359 and compounds without any positively ionizable nitrogen atom (GPV 0360, 0366, 0570). Additionally, also a subset varied according to Topliss [33] was included (GPV 0334, 0335, 0336, 0476, 0608, 0610, 0633, 0636, 0643). Within this extended data set, lipophilicity still plays a role, but is not sufficient to properly describe the data set ($r^2 = 0.48$). Analysing the plot of observed *vs*. predicted $\log(1/EC_{50})$ values clearly shows, that the CoMFA model obtained is able to properly predict pharmacological activity of compounds showing outlier characteristics in the logP/log potency ratio. This may be exemplified by e.g. the diphenylalkylamine GPV 0182 (high logP but low potency) and GPV 0062 (low logP but high potency).

Analysing the results of the CoMSIA study, qualitatively similar conclusions can be drawn. Also in this case, the highest Q^2 value is obtained with a combination of steric and electrostatic fields (0.681). Although it has been clearly demonstrated that for P-gp inhibitors hydrophobicity should be regarded as a space directed property [15,21], the additional use of hydrophobic fields did not improve the results. Also inclusion of logP values as additional descriptor had no beneficial effect on the internal predictivity. However, looking at the contour plots of the hydrophobic fields, a clear positive influence can be seen in the vicinity of the aromatic ring C (Figure 5c). This is in accordance with the pharmacophoric feature model, where in contrast to the features at rings A and B (aromatic) those on ring C were assigned as hydrophobic.

Holographic QSAR

Holographic QSAR (HQSAR) is a new method for generating alignment free QSAR-models. A molecular hologram is derived directly from a connection table and encodes the presence of fragment substructures in a manner analogous to fingerprints. However, in contrast to e.g. UNITY fingerprints, a molecular hologram retains a count of the number of times each bin is set (e.g. 0 3 9 19 0 1 0 15) rather than using a binary bit string (e.g. 0 1 1 1 0 1 0 1). HQSAR is sufficiently fast in execution for screening

Table 3. CoMSIA Models Derived from 119 Propafenone-type P-gp Inhibitors

Model	Q^2	N_{opt}	r^2	SEE
Steric	0.601	2	0.689	0.456
Electrostatic	0.638	15	0.931	0.228
Hydrophobic	0.554	2	0.671	0.469
Steric/Electrostatic	0.681	15	0.942	0.210
Steric/Electrostatic + Hydrophobic	0.595	4	0.768	0.398
Steric + Donor/Acceptor	0.589	6	0.803	0.369
Steric + Hydrophobic	0.592	4	0.745	0.416
Electrostatic + Donor/Acceptor	0.548	7	0.854	0.320
Electrostatic + Hydrophobic	0.564	4	0.766	0.399
Steric/Electrostatic + Donor/Acceptor	0.602	6	0.840	0.332
Steric + logP	0.613	4	0.731	0.428
Electrostatic + logP	0.611	8	0.890	0.279
Steric/Electrostatic + logP	0.640	8	0.891	0.277
Steric/Electrostatic + Hydrophobic + logP	0.606	4	0.758	0.406

medium sized compound libraries and several successful applications have been published [27]. In order to explore the applicability of this new method for analysis of data dealing with more promiscuous ligand/protein interactions, we also performed an HQSAR analysis on our data set. All possible combinations of topological informations used for generating the molecular hologram were explored and the results are presented in Table **4**. Internal predictivity values range from $Q^2 = 0.564$ (using only bonds) to as high as $Q^2 = 0.725$ (connections and hydrogens). This is slightly better than results obtained by 3D-QSAR studies.

The best model was used to analyse the influence of given substructures on the pharmacological activity. This was done by visual inspection of the color coded display of each compound (Figures 6a and 6b). the following main conclusions may be drawn:

-) a basic nitrogen atom is beneficial for activity. This is in agreement with previous findings which showed, that in this region of the molecules H-bond acceptor strength is positively correlated to pharmacological activity. Although this does not necessarily require a positively ionizable nitrogen atom (also amides are strong H-bond acceptors), basic nitrogen atoms can be assumed to act as strong H-bond acceptors. Previously calculations done with HYBOT support this explanation.

-) the beneficial influence of phenyl ring B increases when electron rich systems such as naphthyl, p-methoxy or p-dimethylamino are present. This is in accordance with results obtained when applying a Topliss approach to this aromatic ring system indicating a π-π interaction of this region with the protein [34].

-) a highly negative influence was found for diphenylalkyl-groups in the vicinity of the nitrogen atom, which is a further indication for steric constraints in this region.

Virtual Screening

In principle, HQSAR may also be used for virtual screening of medium sized compound libraries. In contrast to CoMFA and CoMSIA, no alignment is used. Thus, we generated a virtual library of 158 propafenone derivatives based on a Free-Wilson based encoding scheme as published previously [35]. The corresponding molecular holograms were calculated and the biological activity of the compounds was predicted using the five best models derived. A subset of 12 out of these 158 compounds of the virtual library was synthesized and pharmacologically tested to assess the external predictivity of the HQSAR-model. As shown in Table **5**, r^2 values for external predictivity ranged from 0.40 – 0.64 and are thus lower than the internal predictivity. However, calculating the mean values and standard deviations of the five different predictions demonstrated the

Table 4. Results of All Possible Combinations of Informations Used for Generating Molecular Holograms; A Atoms, B Bonds, C Connections, H Hydrogens, D Donor/Acceptor

Inf.	L[a]	C[b]	r^2	Q^2	Inf	L	C	r^2	Q^2
A	53	10	0,808	0,628	*A,B,H*	53	7	0,814	0,696
B	71	9	0,717	0,564	*A,B,D*	71	8	0,839	0,668
C	83	10	0,839	0,679	***A,C,H***	**53**	**10**	**0,84**	**0,715**
H	29	7	0,735	0,680	*A,C,D*	257	10	0,877	0,652
D	37	7	0,799	0,681	***A,H,D***	**43**	**7**	**0,807**	**0,714**
A,B	199	8	0,823	0,636	*B,C,H*	307	10	0,855	0,697
A,C	53	9	0,819	0,662	*B,C,D*	71	8	0,847	0,663
A,H	61	8	0,809	0,698	*B,H,D*	71	5	0,779	0,706
A,D	59	10	0,843	0,702	*C,H,D*	199	7	0,84	0,712
B,C	257	4	0,774	0,646	*A,B,C,H*	43	10	0,844	0,711
B,H	43	7	0,765	0,667	*A,B,C,D*	71	9	0,858	0,660
B,D	71	8	0,838	0,690	*A,B,H,D*	151	5	0,795	0,711
C,H	**97**	**10**	**0,846**	**0,725**	*A,C,H,D*	43	7	0,814	0,706
C,D	353	8	0,86	0,678	*B,C,H,D*	61	9	0,83	0,713
H,D	**353**	**6**	**0,79**	**0,722**	***A,B,C,H,D***	**307**	**8**	**0,855**	**0,716**
A,B,C	151	4	0,763	0,634					

[a] best hologram lenght; [b] number of components

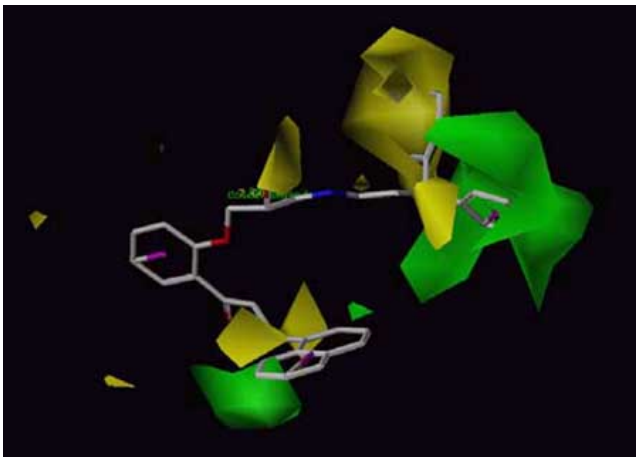

Fig. (5a). Steric contributions of CoMFA fields; green: favorable, yellow: unfavorable.

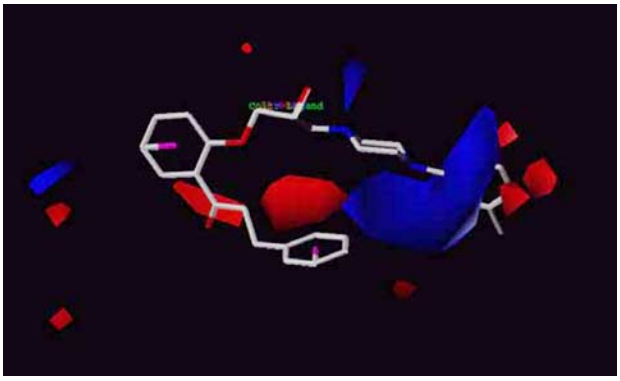

Fig. (5b). Electrostatic contributions of CoMFA fields; blue: low electron density favorable; red: high electron density.

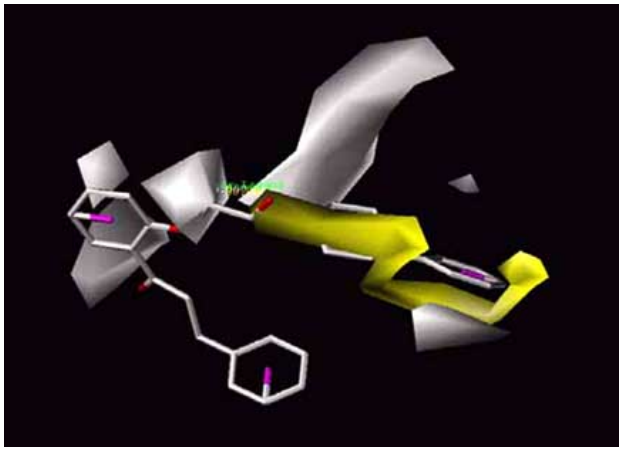

Fig. (5c). Plot of hydrophobic fields from the CoMSIA analysis; yellow: favorable; white: unfavorable.

robustness of the models. The corresponding r^2 values for the correlation of these consensus prediction values with the actual log(potency) values was 0.52, whereby the HQSAR model tended to underpredict the biological activity of the compounds (Figure 7).

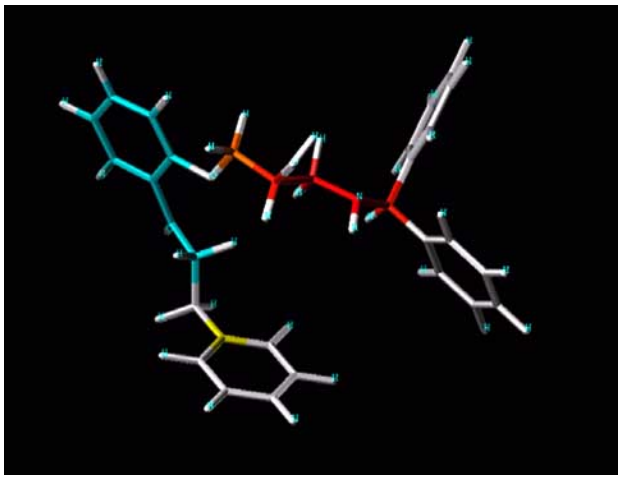

Fig. (6a). HQSAR color coding of the diphenylamine derivative GPV 0182; red: negative contribution to activity; green: positive contribution to activity .

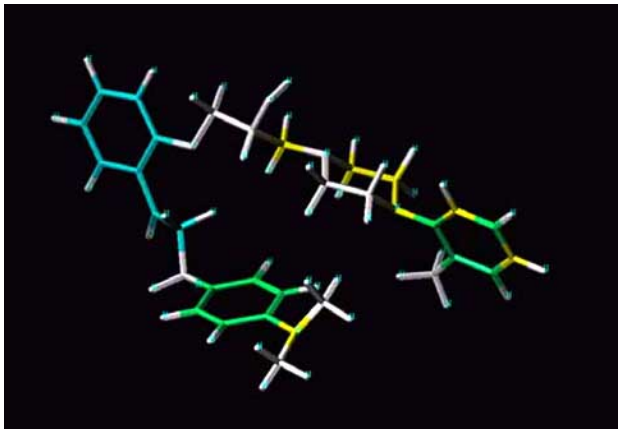

Fig. (6b). HQSAR color coding of the dimethylaminophenyl derivative GPV 0610; green: positive contribution to activity.

When comparing these predictions to those obtained by artificial neural networks (r^2 = 0.64; D. Kaiser, unpublished results), the latter performed substantially better in the external prediction. Studies clarifying the issue whether nonlinear data handling of holograms might improve the external predictivity are currently performed in our group.

CONCLUSIONS

In this study an extended set of propafenone-type inhibitors of P-gp were analyzed by means of 3D-QSAR methods and hologram QSAR. Both CoMFA and CoMSIA yielded highly predictive models, whereby additional use of calculated logP values increased the internal predictivity of the models. Both unfavorable steric and favorable electrostatic and hydrophobic interaction fields were identified, which enabled to explain all outlier identified in previous Hansch-analyses.

Table 5. Predicted and Observed EC_{50}-values of a Set of Compounds Taken from the Virtual Library; the Chemical Structure of the Compounds is Given in Table 1

Code	CH	HD	ABCHD	ACH	AHD	Consens	Actual
DKD 001	0.700	1.884	1.067	1.225	1.403	1.256 ± 0.44	0.188
DKD 004	0.324	0.839	0.989	0.578	1.324	0.811 ± 0.38	0.080
DKD 006	5.470	14.79	8.414	4.266	13.18	9.225 ± 4.64	10.09
DKD 013	3.606	3.548	4.074	3.926	5.358	4.102 ± 0.74	0.836
DKD 014	5.916	10.12	6.095	5.023	9.954	7.421 ± 2.42	4.285
DKD 015	4.529	8.913	6.324	6.081	9.683	7.106 ± 2.13	1.445
DKD 016	3.119	1.581	1.626	2.399	2.786	2.302 ± 0.69	0.121
DKD 024	0.608	0.486	0.467	0.589	0.649	0.560 ± 0.08	0.505
DKD 032	0.017	0.067	0.020	0.015	0.048	0.033 ± 0.02	0.086
DKD 037	5.129	2.692	3.319	4.656	3.990	3.957 ± 0.98	0.178
DKD 039	7.816	8.730	13.34	7.031	10.00	9.382 ± 2.47	3.475
DKD 042	0.471	0.480	0.475	0.397	0.601	0.485 ± 0.07	0.190
r^2-values	0.45	0.64	0.51	0.40	0.54	0.52	

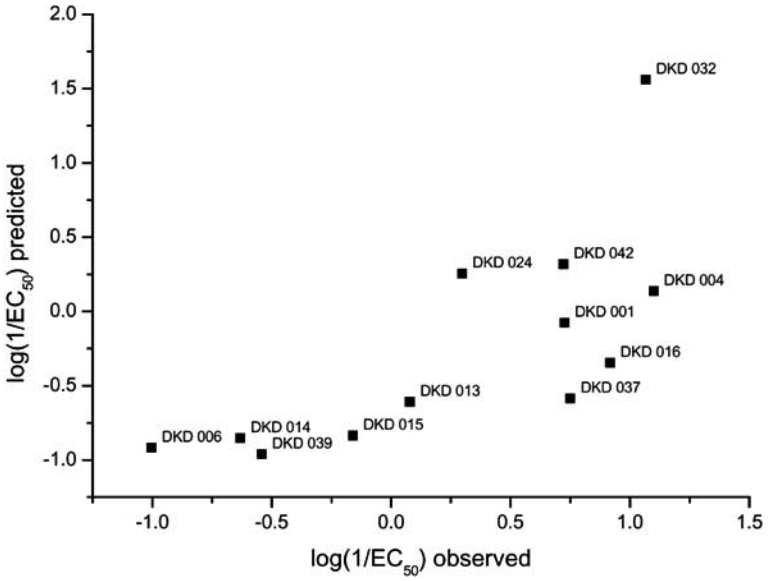

Fig. (7). Plot of observed *vs*. predicted log(1/EC_{50}) values (consensus HQSAR model) for compounds of the virtual library.

In hologram QSAR analysis, positive influences were found for electron donating groups on the aromatic systems, which supports the hypothesis of π-π interactions being involved in ligand binding. Highly negative influences were found for diphenylalkylamine substituents, indicating steric hindrance. The models with highest predictive power were used for screening of a small virtual library. Synthesis and pharmacological testing of a sub set of this library showed, that the external predictivity of the HQSAR models is lower than expected. Comparison with results obtained by artificial neural networks showed, that non-linear relationships seem to be present within the data set. Further studies using also non-linear processing of molecular holograms will show whether combining neural networks with molecular holograms will further improve the external predictivity of the method.

ACKNOWLEDGEMENT

This work was supported by a grant from the Austrian Science Fund (FWF, grant P17014-B11). We are grateful to the Vienna University Computer Center for providing us with the SYBYL molecular modeling software package.

REFERENCES

[1] Ambudkar, S.V.; Dey, S.; Hrycyna, C.A.; Ramachandra, M.; Pastan, I.; Gottesman, M.M. *Annu. Rev. Pharmacol. Toxicol.*, **1999**, *39*, 361.

[2] Gottesman, M.M.; Fojo, T.; Bates, S.E. *Nat. Rev. Cancer*, **2002**, *2*, 48.

[3] St Georgiev, V. *Curr. Drug Targets*, **2000**, *1*, 261.

[4] Li, X.Z.; Nikaido, H. *Drugs*, **2004**, *64*, 159.

[5] Kerboeuf, D.; Blackhall, W.; Kaminsky, R.; von Samson-Himmelstjerna, G. *Int. J. Antimicrob. Agents*, **2003**, *22*, 332.

[6] Szakacs, G.; Annereau, J.P.; Lababidi, S.; Shankavaram, U.; Arciello, A.; Bussey, K.J.; Reinhold, W.; Guo, Y.; Kruh, G.D.; Reimers, M.; Weinstein, J.N.; Gottesman, M.M. *Cancer Cell*, **2004**, *6*, 129.

[7] Begley, D.J. *Curr. Pharm. Des*., **2004**, *10*, 1295.

[8] Dietrich, C.G.; Geier, A.; Elferink, R.P. *Gut*, **2003**, *52*, 1788.

[9] Robert, J.; Jarry, C. *J. Med. Chem*., **2003**, *46*, 4805.

[10] Pleban, K.; Ecker, G.F. *Mini-Rev. Med. Chem*., **2005**, *5*, 29.

[11] Lin, J.H.; Yamazaki, M. *Drug Metab. Rev*., **2003**, *35*, 417.

[12] Chiba, P.; Ecker, G.F. *Expert Opin. Ther. Patents*, **2004**, *14***,** 499.

[13] Potschka, H.; Fedrowitz, M.; Loscher, W. *Neurosci. Lett*., **2002**, *26*, 173.

[14] Avendano, C.; Menendez, J.C. *Curr. Med. Chem*. **2002**, 9, 159.

[15] Pajeva, I. K.; Wiese, M. *Quant. Struct.-Act. Relat.,* **1998**, *17*, 301.

[16] Pajeva, I.; Wiese, M. *J. Med. Chem*., **1998**, *41*, 1815.

[17] Ekins, S.; Kim, R.B.; Leake, B.F.; Dantzig, A.H.; Schuetz, E.G.; Lan, L.; Yasuda, K.; Shepard, R.L.; Winter, M.A.; Schuetz, J.D.; Wikel, J.H.; Wrighton, S.A. *Mol. Pharmacol*., **2002**, *61*, 974.

[18] Pajeva, I.K.; Wiese, M. *J. Med. Chem*., **2002**, *45*, 5671.

[19] Langer, T.; Eder, M.; Hoffmann, R.D.; Chiba, P.; Ecker, G.F. *Arch. Pharm. Pharm. Med. Chem*., **2004**, *337***,** 317.

Received: 05 October, 2004 Accepted: 11 April, 2005

[20] Klein, C.; Kaiser, D.; Kopp, S.; Chiba, P.; Ecker, G.F. *J. Comput. Aided Molecular Drug Design*, **2002**, *16*, 785.

[21] Pleban, K.; Hoffer, C.; Kopp, S.; Peer, M.; Chiba, P.; Ecker, G.F. *Arch. Pharm. Pharm. Med. Chem*., **2004**, *337*, 328.

[22] Chiba, P.; Rebitzer, S.; Richter, E.; Hitzler, M.; Ecker, G. *Bioorg. Med. Chem. Lett*., **1998**, *8*, 829.

[23] Ecker, G.; Huber, M.; Schmid, D.; Chiba, P. *Mol. Pharmacol*., **1999**, *56*, 791.

[24] Molecular Networks GmbH, Naegelbachstr. 25, 91052 Erlangen, Germany (http://www. mol-net.de).

[25] Cambridge Crystallographic Data Centre: http://www.ccdc.cam.ac.uk

[26] Tripos GmbH, Martin-Kollar Strasse 13, D-81829 Muenchen, Germany (http://www.tripos.com).

[27] Winkler, D.A.; Burden, F.R. *Quant. Struct.-Act. Relat*., **1998**, *17*, 224.

[28] Boer, R.; Gekeler, V.; Ulrich, W.R.; Zimmermann, P.; Ise, W.; Schodl, A.; Haas, S. *Eur. J. Cancer,* **1996**, *32A***,** 857.

[29] Ecker, G.F.; Csaszar, E.; Kopp, S.; Plagens, B.; Holzer, W.; Ernst, W.; Chiba, P. *Mol. Pharmacol*., **2002**, *61***,** 637.

[30] Ecker, G.; Chiba P. *Recent Res. Devel. Medicinal Chem.*, **2001**, *1*, 121.

[31] Klopman, G.; Shi, L. M.; Ramu, A. *Mol. Pharmacol*., **1997**, *52*, 323.

[32] Chiba, P.; Ecker, G.; Schmid, D.; Drach, J.; Tell, B.; Goldenberg, S.; Gekeler, V. *Mol. Pharmacol*., **1996**, *49*, 1122.

[33] Topliss, J.G. *J. Med. Chem*., **1977**, *20*, 463.

[34] Tmej, C.; Richter, E.; Hitzler, M.; Chiba, P.; Ecker, G.; Fleischhacker, W. *J. Pharm. Pharmacol*., **1997**, *49 (Suppl. 4)*, 106.

[35] Kaiser, D.; Tmej, C.; Chiba, P.; Schaper, K.-J.; Ecker, G. *Sci. Pharm*., **2000**, *68*, 57.